Carbohydrate Research, 233 (1992) 15–34
Elsevier Science Publishers B.V., Amsterdam

Conformational analysis of the anomeric forms of sophorose, laminarabiose, and cellobiose using MM3

Michael K. Dowd [a], Alfred D. French [b] and Peter J. Reilly [a]

[a] *Department of Chemical Engineering, Iowa State University, Ames, Iowa 50011 (USA)*
[b] *Southern Regional Research Center, U.S. Department of Agriculture, New Orleans, Louisiana 70179 (USA)*

(Received December 12th, 1991; accepted February 7th, 1992)

ABSTRACT

Relaxed-residue energy maps based on the MM3 force-field were computed for relative orientations of the pyranosyl rings of sophorose, laminarabiose, and cellobiose, respectively the (1 → 2)-β-; (1 → 3)-β-; and (1 → 4)-β-linked D-glucosyl disaccharides. Sixteen starting conformations of the rotatable exocyclic side-groups were considered for each molecule. All of the energy surfaces have two intersecting low-energy troughs and illustrate the importance of exo-anomeric effects in determining disaccharide conformation. Local minima were found by relaxed minimization without restriction. The energy surfaces of these disaccharides are very similar to the energy surfaces of their corresponding 6-methyltetrahydropyran analogues. There is good agreement between disaccharide structures having minimal MM3 energy and those found by crystallography.

INTRODUCTION

In the past several years, there has been much interest in modelling conformations of cellobiose, the disaccharide subunit of cellulose fibers[1–7]. Early studies attempted either to isolate the low-energy minima or to compute energy surfaces relative to the glycosidic torsional angles based on rigid monomer geometries[1–3]. Computational advances now enable disaccharides to be studied with all degrees of freedom completely relaxed. Comparative studies using rigid versus relaxed monomers have shown that this change produces markedly different energy maps, with far more conformational freedom being afforded disaccharides by relaxed monomers[4–6]. In contrast to cellobiose, there has been relatively little interest in modelling the other β-linked disaccharides. Only the early reports of Sathyanarayana and Rao, based on rigid monomer unit techniques, have compared the conformational freedom of the (1 → 2)-, (1 → 3)-, and (1 → 4)-linked D-glucosyl

Correspondence to: Dr. P.J. Reilly, Department of Chemical Engineering, Iowa State University, Ames, IA 50011, USA.

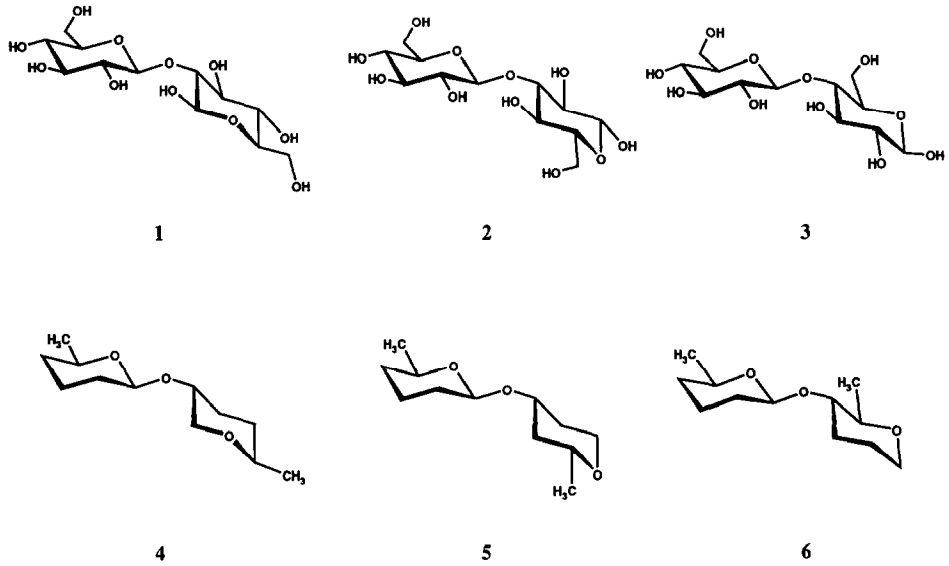

Fig. 1. Structures of β-sophorose (**1**), β-laminarabiose (**2**), β-cellobiose (**3**), and equatorially–equatorially linked 3-(6-methyltetrahydropyran-2-yloxy)-6-methyltetrahydropyran (**4**), 4-(6-methyltetrahydropyran-2-yloxy)-6-methyltetrahydropyran (**5**), and 5-(6-methyltetrahydropyran-2-yloxy)-6-methyltetrahydropyran (**6**).

disaccharides[8,9]. For the three equatorially–equatorially linked species, their potential function yielded global minima in different regions, with the differences attributed to hydrogen bonding, since the minima were found in the same region when these interactions were neglected[8]. To some degree this contrasts with recent work based on relaxed-residue modelling of disaccharides, where hydrogen bonding is of secondary importance in determining general map appearance[10,11].

In this study, relaxed-residue techniques have been used to study the conformational characteristics of sophorose [D-glucopyranosyl-(1 → 2)-β-D-glucose, Fig. 1, **1**]; laminarabiose [D-glucopyranosyl-(1 → 3)-β-D-glucose, **2**]; and cellobiose [D-glucopyranosyl-(1 → 4)-β-D-glucose, **3**], as well as the 6-methyltetrahydropyran analogues of these disaccharides. Comparisons are made between the modelling results and reported crystal structures for each of the three molecules. This work complements our previous articles on the (1 → 1)-, (1 → 2)-α-, (1 → 3)-α-, and (1 → 4)-α-linked D-glucosyl disaccharides[10,11].

COMPUTATIONAL METHODS

The computational methods used in this project have been described in detail elsewhere and will only be summarized here[10,11]. Torsional angles representing the orientations of the rings about the glycosidic bonds are defined as ϕ = H(C-1)–C-1–O-1–C-i' and ψ = C-1–O-1–C-i'–H(C-i'), where i' represents the 2′, 3′, or 4′

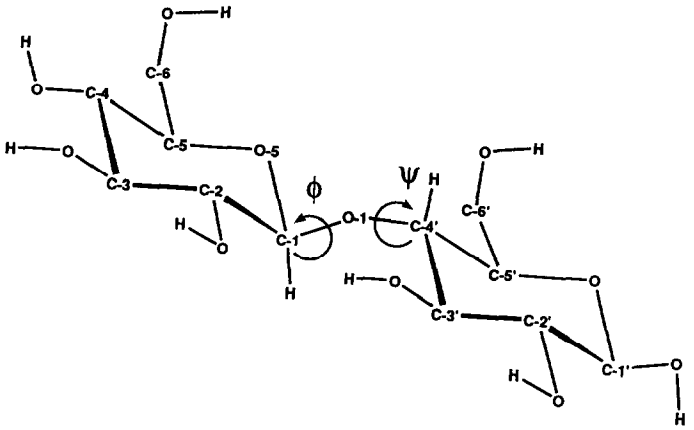

Fig. 2. Definition of the torsional angles ϕ and ψ in β-cellobiose.

carbon atoms of the reducing ring (Fig. 2). MM3 (January 22, 1990 update), developed by Allinger[12–14] and marketed by the Technical Utilization Corporation, Powell, OH, was used in this study. The MM3 dielectric constant (ϵ) was set to 4.0 for all calculations, as this has been found most appropriate from comparisons of the D-glucopyranose ring with crystal structures[15]. No attempt was made to account for solvation. The block diagonal minimization method, with the default convergence criterion (3.6 cal/mol), was used for grid-point optimizations, and all maps, unless noted, were constructed on a 20° grid spacing.

Sixteen starting structures were used at each ϕ, ψ point for each disaccharide. These structures were all composed of $^4C_1$ D-glucopyranose rings, but varied in the conformations of exocyclic side-groups. The hydroxymethyl groups had either *gauche–gauche* (*gg*) or *gauche–trans* (*gt*) orientations (relative to the ring C-4 and O-5 atoms, respectively), with their hydroxyl hydrogen atoms oriented to weakly hydrogen bond with the ring oxygen atoms. *trans–gauche* Hydroxymethyl orientations (*tg*) were not considered, since they are not found in structures determined by single-crystal methods[16] or as significant conformers in solution[17,18], and have higher energies calculated by MM3 at $\epsilon = 4.0$ (work in progress). Clockwise (*c*) and reverse-clockwise (*r* or *r'*) orientations of the secondary hydroxyl groups were considered (Table I), as has been discussed before[11,19]. For the reverse-clockwise orientation, the torsional angle C-3'–C-2'–O-2'–H(O-2') is 60° for α anomers (*r'*) and 180° for β anomers (*r*). These orientations place H(O-2') in favorable positions to continue a ring of cooperative hydrogen bonds around the pyranose ring.

At each grid-point the lowest energy value from the sixteen optimized starting conformations was used to prepare the maps. Isoenergy contour lines were generated using the routines available within DISSPLA Graphics, Release 11.0 (Computer International, Garden City, NY). After finding the general location of

TABLE I

Approximate angles (±5°) used for clockwise (*c*) and reverse-clockwise (*r* and *r'*) torsional orientations of the secondary hydroxyl groups

Torsional angle (deg)	α Anomer			β Anomer	
	c	*r*	*r'*	*c*	*r*
Nonreducing ring					
H(O-2)–O-2–C-2–C-3	−60	180		−60	180
H(O-3)–O-3–C-3–C-4	60	180		60	180
H(O-4)–O-4–C-4–C-5	−60	180		−60	180
Reducing ring					
H(O-1')–O-1'–C-1'–C-2'	−60		180	60	180
H(O-2')–O-2'–C-2'–C-3' [a]	−60		60	−60	180
H(O-3')–O-3'–C-3'–C-4' [b]	60		180	60	180
H(O-4')–O-4'–C-4'–C-5' [c]	−60		180	−60	180

[a] Not applicable for sophorose. For this disaccharide, *r* and *r'* are identical conformations when referenced to the reducing ring. [b] Not applicable for laminarabiose. [c] Not applicable for cellobiose.

the energy minima, final structures were obtained by full-matrix optimization as described in a previous article[11]. From the population of optimized structures, a molecular partition function *q* is defined as

$$q = \sum_{\phi,\psi} \exp[-E(\phi, \psi)/RT]$$

where $E(\phi, \psi)$ is the Boltzmann-averaged energy calculated from the optimized 16 starting conformations, *R* is the gas constant, and *T* is the temperature. This gives a concise method of describing the extent of rotational freedom about the glycosidic and aglycon bonds, and an average energy is calculated based on this function for each disaccharide[11].

Conformational maps were also generated for the 6-methyltetrahyropyran analogues of sophorose, laminarabiose, and cellobiose: equatorially–equatorially linked 3-(6-methyltetrahydropyran-2-yloxy)-6-methyltetrahydropyran (Fig. 1, **4**), 4-(6-methyltetrahydropyran-2-yloxy)-6-methyltetrahydropyran (**5**), and 5-(6-methyltetrahydropyran-2-yloxy)-6-methyltetrahydropyran (**6**), respectively. Similar analogues have been used in past computational studies as carbohydrate models[10,11,20]. The lack of hydroxyl groups for these analogues eliminates the need to consider multiple starting conformations, and therefore the maps were constructed on a 10° grid spacing. The starting models of the tetrahydropyran rings had $^5C_2$ ring conformations, equivalent to the $^4C_1$ form of D-glucosyl rings.

RESULTS

α- and β-Sophorose.—The MM3 maps of α- and β-sophorose are shown in Fig. 3, with isoenergy contour lines at 1 kcal/mol increments above the global minimum and the local minima denoted. Signs of two perpendicularly intersecting

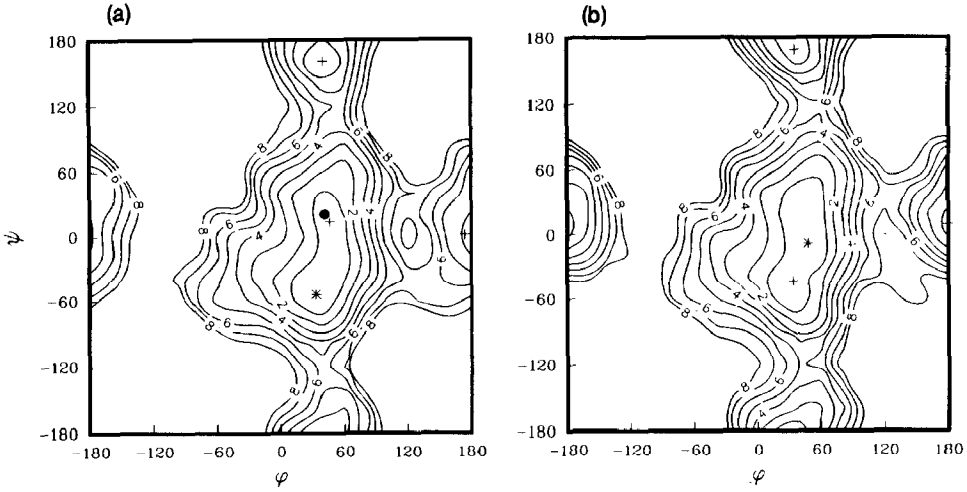

Fig. 3. MM3-generated relaxed-residue steric energy maps of α-sophorose (a) and β-sophorose (b). Contour lines are graduated in 1-kcal/mol increments above the global minimum: (∗) global MM3 minima; (+) local MM3 minima; (●) α-sophorose hydrate crystal conformer[32].

troughs appear on the maps, although some of the energy barriers between low-energy regions are larger than 8 kcal/mol. Table II list the MM3 energies and locations of the minima found within the contoured regions. The two lowest energy minima lie in a trough defined by the 1 kcal/mol contour that extends in the ψ-direction from approximately $-60°$ through 60°. For α-sophorose, two minima are found at ϕ, $\psi = 33°$, $-54°$ and ϕ, $\psi = 46°$, 14°, one to each side of the eclipsed orientation of $\psi = 0°$. The former minimum is lower in energy by 0.6 kcal/mol. For β-sophorose the two lowest energy minima are at ϕ, $\psi = 48°$, $-8°$ and ϕ, $\psi = 34°$, $-43°$. The energy differences between the two minima are very small. Two additional minima also occur on each map. The third lowest is found along the trough aligned in the ψ-direction at ϕ, $\psi = 40°$, 161° for α-sophorose and ϕ, $\psi = 35°$, 169° for β-sophorose. The last minimum is in the second trough at ϕ, $\psi = 174°$, 1° and ϕ, $\psi = 180°$, 9° for α- and β-sophorose, respectively.

Table III shows the importance of individual starting conformations to the final points for the whole map, as well as for the region enclosed by the 8 kcal/mol contour lines. Fig. 4 shows the pattern of starting conformations that contribute to the final map, with contour lines overlaid at 2 kcal/mol intervals above the global minimum. The *gt* orientation of the hydroxymethyl groups contributes most of the final map points, as occurs for MM3 modelling of other D-glucosyl disaccharides[10,11]. Within the region defined by the 2 kcal/mol contour, only *gt*-derived structures are found. The initial secondary hydroxyl groups contribute most when both rings are aligned in a reverse-clockwise (*r* or *r'*) orientation, although mixed orientations also occur to a significant degree. As the *r* and *r'* orientations differ in only one hydroxyl orientation, transitions between the two forms during the minimization process are likely.

TABLE II

Steric energy minima for MM3-calculated relaxed-residue analysis of sophorose, laminarabiose, and cellobiose

Disaccharide	Location of minimum		Initial conformer	Relaxed energy (kcal/mol)
	ϕ	ψ		
α-Sophorose	33.4	−54.2	*gtggrc*	21.47
	46.2	13.7	*gtgtrr'*	22.07
	40.4	160.8	*gtgtrr'*	23.59
	173.8	1.4	*gtgtrr'*	25.19
β-Sophorose	48.0	−8.3	*gtgtrc*	21.45
	34.0	−43.4	*gtgtrc*	21.48
	35.2	169.2	*gtgtrr*	22.73
	179.8	9.3	*gtgtrr*	23.25
α-Laminarabiose	35.4	−48.1	*gtgtrc*	20.99
	36.3	169.2	*gtggrc*	23.93
	179.6	10.8	*gtggrc*	24.34
β-Laminarabiose	35.0	−42.3	*gtgtrr*	20.15
	48.5	−9.0	*gtgtrr*	20.18
	36.2	168.8	*gtggrc*	23.76
	177.3	12.4	*gggtcc*	24.34
α-Cellobiose	50.4	−10.7	*gtgtrc*	20.30
	35.8	−46.0	*gtgtrc*	20.37
	37.8	172.2	*gtgtrc*	22.94
	−179.4	0.7	*ggggrr'*	24.73
β-Cellobiose	36.0	−46.2	*gtgtrc*	20.26
	50.5	−10.7	*gtgtrc*	20.29
	34.4	172.3	*gtgtrr*	22.34
	−179.4	0.8	*ggggrr*	23.85

The calculated partition function for each anomer is shown in Table IV and indicates that β-sophorose has more conformational freedom about the glycosidic linkages. The 0.5 kcal/mol contour line (not shown) occupies a much larger region on the β-sophorose map and is consistent with the large difference in partition function between the two anomers. The (1 → 2)-α-linked disaccharide kojibiose also shows a large difference between its two anomeric forms for this function[11]. This also illustrates that significant differences in modelled properties of disaccharides can result from relatively small structural changes such as anomeric orientation. The average energy calculated from the partition function is lower for α-sophorose; hence an equilibrium gas-phase mixture of the two anomeric forms would favor this anomer. Experimental determinations of the anomeric ratio in deuterium oxide[21], water[22], and pyridine[23] also favor α-sophorose.

α- and β-Laminarabiose.—The MM3 maps for α- and β-laminarabiose are shown in Fig. 5. A region of less than 2 kcal/mol above the global minimum runs parallel to the ψ-axis between −60° and 60°, as with sophorose. The global minima

TABLE III

Starting structures contributing to MM3-generated relaxed-residue ϕ, ψ disaccharide maps

Disaccharide	Complete map		Lowest 8 kcal/mol		
	Hydroxy-methyl (%)	Secondary hydroxyls (%)	Area of map (%)	Hydroxy-methyl (%)	Secondary hydroxyls (%)
α-Sophorose	*gggg* (0.9)	*cc* (3.4)	46.3	*gggg* (0.7)	*cc* (0.7)
	gggt (6.2)	*cr'* (23.5)		*gggt* (5.3)	*cr'* (12.0)
	gtgg (10.5)	*rc* (21.9)		*gtgg* (10.7)	*rc* (18.0)
	gtgt (82.4)	*rr'* (51.2)		*gtgt* (83.3)	*rr'* (69.3)
	Total representation of conformers:				
	14 of 16		10 of 16		
β-Sophorose	*gggg* (0.3)	*cc* (7.1)	45.4	*gggg* (0.0)	*cc* (1.4)
	gggt (5.6)	*cr* (16.7)		*gggt* (3.4)	*cr* (6.8)
	gtgg (0.6)	*rc* (19.4)		*gtgg* (0.7)	*rc* (17.7)
	gtgt (93.5)	*rr* (56.8)		*gtgt* (95.9)	*rr* (74.1)
	Total representation of conformers:				
	9 of 16		6 of 16		
α-Laminarabiose	*gggg* (3.4)	*cc* (17.6)	38.0	*gggg* (1.6)	*cc* (6.5)
	gggt (5.0)	*cr'* (8.0)		*gggt* 1.6)	*cr'* (1.6)
	gtgg (33.0)	*rc* (39.5)		*gtgg* (39.9)	*rc* (48.0)
	gtgt (58.6)	*rr'* (34.9)		*gtgt* (56.9)	*rr'* (43.9)
	Total representation of conformers:				
	13 of 16		9 of 16		
β-Laminarabiose	*gggg* (0.9)	*cc* (14.5)	35.2	*gggg* (0.0)	*cc* (6.1)
	gggt (6.2)	*cr* (16.1)		*gggt* (7.0)	*cr* (3.5)
	gtgg (17.3)	*rc* (21.9)		*gtgg* (16.7)	*rc* (21.1)
	gtgt (75.6)	*rr* (47.5)		*gtgt* (76.3)	*rr* (69.3)
	Total representation of conformers:				
	14 of 16		10 of 16		
α-Cellobiose	*gggg* (3.1)	*cc* (25.0)	30.9	*gggg* (5.0)	*cc* (10.0)
	gggt (7.1)	*cr'* (4.6)		*gggt* (0.0)	*cr'* (2.0)
	gtgg (18.8)	*rc* (50.6)		*gtgg* (34.0)	*rc* (67.0)
	gtgt (71.0)	*rr'* (19.8)		*gtgt* (61.0)	*rr'* (21.0)
	Total representation of conformers:				
	13 of 16		8 of 16		
β-Cellobiose	*gggg* (2.2)	*cc* (19.1)	32.7	*gggg* (3.8)	*cc* (1.0)
	gggt (8.0)	*cr* (7.4)		*gggt* (0.0)	*cr* (2.8)
	gtgg (19.4)	*rc* (31.2)		*gtgg* (33.0)	*rc* (37.7)
	gtgt (70.4)	*rr* (42.3)		*gtgt* (63.2)	*rr* (58.5)
	Total representation of conformers:				
	14 of 16		7 of 16		

for the two anomers are in this region, for α-laminarabiose at ϕ, $\psi = 35°$, $-48°$ and for β-laminarabiose at ϕ, $\psi = 35°$, $-42°$, with the MM3 energy of the latter minimum being lower by 0.84 kcal/mol. Another minimum for β-laminarabiose, only slightly higher in energy, is located within the same 2 kcal/mol region at ϕ, $\psi = 48°$, $-9°$. No equivalent minimum occurs for α-laminarabiose. Other higher-

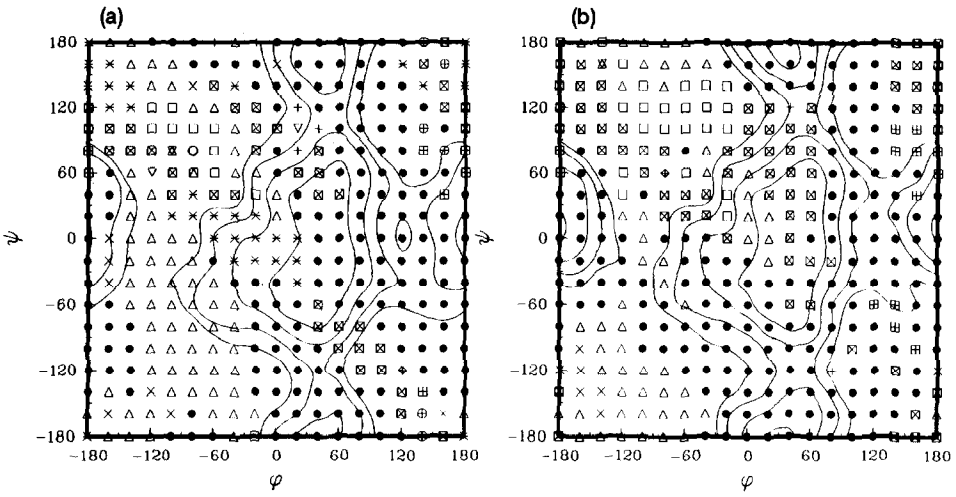

Fig. 4. Distribution of the starting conformations that contribute to the final relaxed-residue maps of α-sophorose (a) and β-sophorose (b). Starting conformations are: *ggggrc* (▽); *ggggrx* (⊕); *gggtcc* (⊠); *ggtcx* (×); *gggtrc* (⊕); *gggtrx* (⊞); *gtggcc* (○); *gtggcx* (⊡); *gtggrc* (✳); *gtggrx* (+); *gtgtcc* (□); *gtgtcx* (△); *gtgtrc* (⊠); *gtgtrx* (●). For the reducing ring the secondary hydroxyl orientation x is defined as r' for α-sophorose and r for β-sophorose. Contour lines are graduated in 2-kcal/mol increments above the overall energy minimum.

energy minima are located in different low-energy regions of the ϕ, ψ maps. The third minimum is at ϕ, $\psi = 36°$, 169° for both anomeric forms, while the fourth minimum is found at ϕ, $\psi = 180°$, 11° for α-laminarabiose and at ϕ, $\psi = 177°$, 12° for β-laminarabiose.

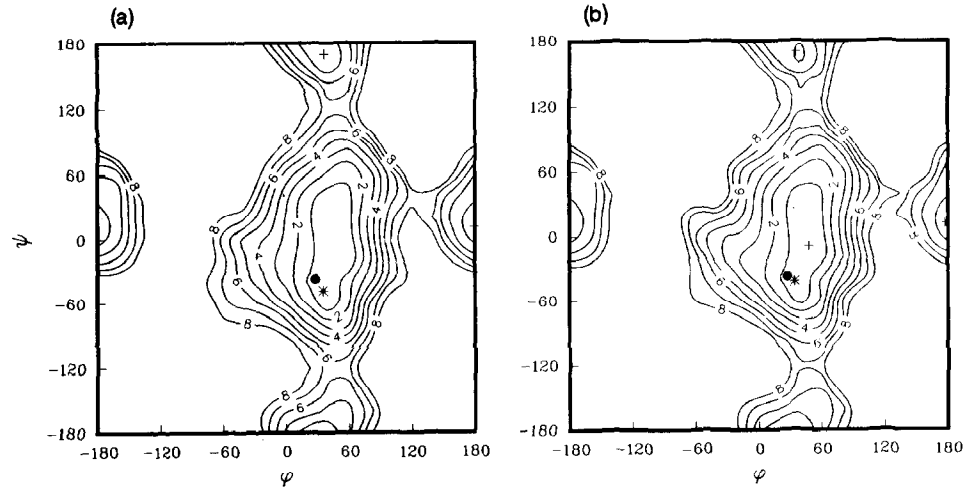

Fig. 5. MM3-generated relaxed-residue steric energy maps of α-laminarabiose (a) and β-laminarabiose (b). Contour lines are graduated in 1-kcal/mol increments above the global minimum: (✳) global MM3 minima; (+) local MM3 minima; (●) laminarabiose hydrate crystal conformer[34].

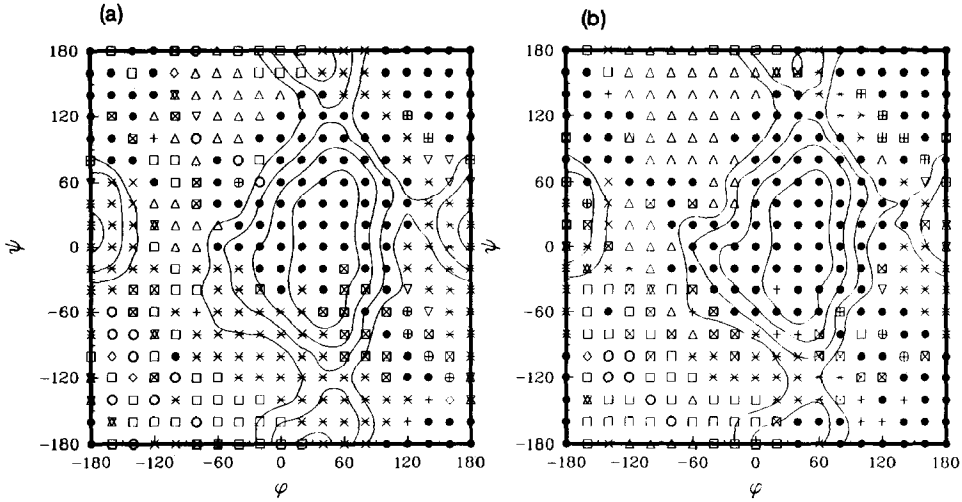

Fig. 6. Distribution of the starting conformations that contribute to the final relaxed-residue maps of α-laminarabiose (a) and β-laminarabiose (b). Starting conformations are: *ggggcc* (◇); *ggggrc* (▽); *gggtcc* (⧆); *gggtcx* (×); *gggtrc* (⊕); *gggtrx* (⊞); *gtggcc* (○); *gtggcx* (⧈); *gtggrc* (✳); *gtggrx* (+); *gtgtcc* (□); *gtgtcx* (△); *gtgtrc* (⊠); *gtgtrx* (●). For the reducing ring the secondary hydroxyl orientation *x* is defined as *r'* for α-laminarabiose and *r* for β-laminaribiose. Contour lines are graduated in 2-kcal/mol increments above the global minimum.

Table III shows the distribution of the sixteen starting conformations of each anomer included in this study, while Fig. 6 presents ϕ, ψ maps identifying the contributing conformers at each grid-point. Only small changes in the conformer distributions are seen between the anomeric forms. The most important starting hydroxymethyl orientation is *gtgt*, which yields more than half the grid points for the whole map and for regions within the the 8 kcal/mol contour. All four combinations of secondary hydroxyl orientations contribute to the final map, with the most important being the *rr* (or *rr'*) and *rc* orientations. The conformational partition function is approximately the same for each anomeric form. The average MM3 energy is lower for β-laminarabiose, indicating that a gas-phase equilibrium mixture would favor it. β-Laminarabiose, measured by NMR spectroscopy, is also favored in deuterium oxide[21]. This ratio has also been investigated in water and pyridine by gas chromatography, but individual peak assignments were not reported[22,23]. Based on NMR results and agreement with the conformational analysis, the larger laminarabiose peak of Nikolov and Reilly is β-laminarabiose[23].

α- and β-Cellobiose.—Maps for α- and β-cellobiose are shown in Fig. 7. As seen for the above disaccharides and from other modelling studies on cellobiose[1–4], the map has two perpendicular low-energy troughs. The contour 2 kcal/mol above the global minimum defines as trough between ψ values of $-60°$ and 40°. Within this trough, two minima occur for each anomer, with the global minima at ϕ, $\psi = 50°$, $-11°$ for α-cellobiose and at ϕ, $\psi = 36°$, $-46°$ for β-cellobiose. The global minimum of β-cellobiose has a slightly lower (< 0.05 kcal/mol) relative

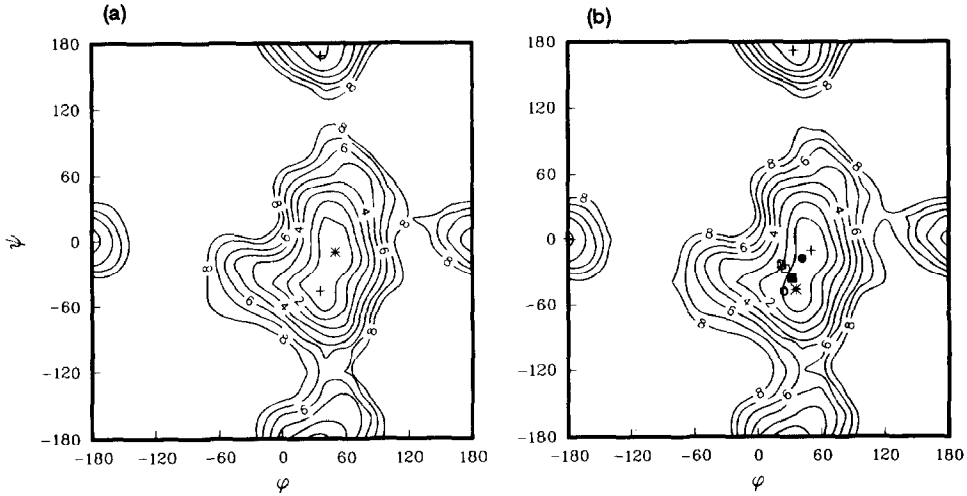

Fig. 7. MM3-generated relaxed-residue steric energy maps of α-cellobiose (a) and β-cellobiose (b). Contour lines are graduated in 1-kcal/mol increments above the global minimum: (✳) global MM3 minima; (+) local MM3 minima; (●[29]) β-cellobiose crystal conformer; (○[30]) methyl-β-cellobiose–methanol crystal conformer; (□[32], ■[33], ⊠[34]): cellobiose conformers from fiber diffraction studies.

energy than the α-cellobiose structure. The other minima in this low-energy region are at ϕ, $\psi = 36°$, $-46°$ for α-cellobiose and at ϕ, $\psi = 50°$, $-11°$ for β-cellobiose. The energy differences between the overall and second minima are also very small (< 0.1 kcal/mol) for each anomer. Two additional minima for each anomer are found within 4.5 kcal/mol of their overall minima. The third is at ϕ, $\psi = 38°$, 172° and ϕ, $\psi = 34°$, 172° for α- and β-cellobiose, respectively, while the fourth occurs at ϕ, $\psi = -179°$, 1° for both cellobiose anomers.

Again the *gt* starting orientation of both hydroxymethyl groups produces the most map points (Table III). All orientations of the secondary hydroxyl groups contribute to the adiabatic maps, with the reverse-clockwise (*rr* or *rr'*) and the mixed reverse-clockwise-clockwise (*rc*) orientations occurring most frequently. Fig. 8 shows the distribution of the contributing conformers on the ϕ, ψ maps. The partition function values (Table IV) show that there is approximately equal conformational freedom about the glycosidic linkages of the two anomers. α-Cellobiose has the slightly lower average energy, despite the slightly lower global minimum of β-cellobiose. In pyridine the experimentally determined anomeric concentrations are almost equal[23]. In contrast, the equilibrium ratios in deuterium oxide[21] and water[22,24] favor β-cellobiose. The range of experimental differences found in different solvents as well as the small calculated energy differences between the two anomers suggest that solvent effects are important in determining this ratio. Tvaroška showed that the effect of solvation energy on MM2-generated β-cellobiose minima can vary between the different minima in the same solvent[25]. Hence, solvent effects might be expected to change the relative appearance of the

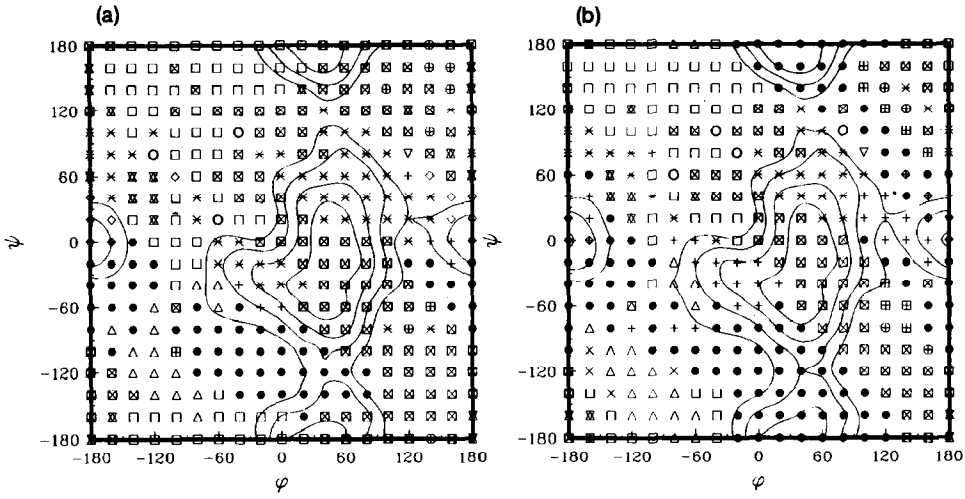

Fig. 8. Distribution of the starting conformations that contribute to the final relaxed-residue maps of α-cellobiose (a) and β-cellobiose (b). Starting conformations are: *ggggcc* (◇); *ggggrc* (▽); *ggggrx* (⊕); *gggtcc* (⊠); *gggtcx* (✳); *gggtrc* (⊕); *gggtrx* (⊞); *gtggcc* (○); *gtggcx* (⊡); *gtggrc* (✕); *gtggrx* (+); *gtgtcc* (□); *gtgtcx* (△); *gtgtrc* (⊠); *gtgtrx* (●). For the reducing ring the secondary hydroxyl orientation *x* is defined as *r'* for α-cellobiose and *r* for β-cellobiose. Contour lines are graduated in 2-kcal/mol increments above the global minimum.

maps. A useful investigation would be an expanded computational study that includes solvation over entire map surfaces for both anomers to test how well anomeric ratios found in different solvents can be reproduced.

Comparison among equatorially–equatorially linked disaccharides.—Similarities are apparent among these disaccharide maps. Two perpendicularly intersecting low-energy troughs occur on each map, although the energy barriers between some of the low-energy regions are higher than 8 kcal/mol. The low-energy trough aligned with the ψ-axis and dependent on the ϕ-torsional angle is centered to the positive side of $\phi = 0°$, which is an expression of the exo-anomeric effect. In contrast, the apparent trough associated with the ψ-torsional angle, which is not

TABLE IV

Molecular partition function (q) and Boltzmann-averaged MM3 energy for equatorially–equatorially linked disaccharides

Disaccharide	q	Average energy (kcal/mol)
α-Sophorose	5.8	22.88
β-Sophorose	8.1	23.43
α-Laminarabiose	6.2	22.10
β-Laminarabiose	6.0	21.33
α-Cellobiose	4.2	21.51
β-Cellobiose	4.0	21.71

directly influenced by an O–C–O segment, is centered roughly at the eclipsed orientation of $\psi = 0°$. Relaxed maps of β,β-trehalose[10], which has an equatorial–equatorial glycosidic bond, and previously reported maps of cellobiose[4–7] show similar traits.

Differences among the disaccharides are apparent in local regions of the maps. For both sophorose and laminarabiose, the 1 kcal/mol contour line encompasses a relatively large region that runs from $\phi = -60°$ over the eclipsed conformation at $\phi = 0°$ and extends towards $\phi = 60°$. For cellobiose this region is much compressed. In addition, many of the energy barriers between minima appear higher for cellobiose than for laminarabiose and sophorose, as is indirectly expressed by the percentage of ϕ, ψ-space occupied within the 8 kcal/mol contour lines. Possibly because the barriers are lower for sophorose, a distinct peak is seen near ϕ, $\psi = 120°$, 0° that is not apparent with the 8 kcal/mol contour on the other disaccharide maps.

For the β anomers, the partition functions suggest that the conformational flexibility is in the order sophorose > laminarabiose > cellobiose. This corresponds structurally with the distance of the hydroxymethyl group from the glycosidic region. The 8 kcal/mol contour lines (Table III) also suggest this result, although the order predicted by Sathyanarayana and Rao based on contact criteria using rigid monomer units is laminarabiose > cellobiose > sophorose[8]. For the α anomers the partition function predicts a conformational flexibility of laminarabiose ≥ sophorose > cellobiose. The change in order occurs because of the large anomeric effect associated with the partition coefficient for sophorose, which has glycosidic and anomeric regions juxtaposed.

Comparison with MM3 modelling of 6-methyltetrahydropyran analogues.—MM3 adiabatic maps were also calculated for the equatorially–equatorially linked tetrahydropyran analogues of sophorose [3-(6-methyltetrahydropyran-2-yloxy)-6-methyltetrahydropyran], laminarabiose [4-(6-methyltetrahydropyran-2-yloxy)-6-methyltetrahydropyran], and cellobiose [5-(6-methyltetrahydropyran-2-yloxy)-6-methyltetrahydropyran]. These maps are shown in Fig. 9, and the localized minima are given in Table V. The two perpendicularly intersecting low-energy troughs generally found for equatorially–equatorially linked disaccharides are also found on the analogue maps. Minima are found in similar regions as those of the disaccharides, and additional minima occur in relatively high-energy plateau regions. As was found for the axially–equatorially linked D-glucosyl disaccharide series, the similarity of these analogue maps suggests that exo-cyclic components have a secondary influence on the map appearance and that the linkage orientation (axial or equatorial) appears to be most important. The sophorose and laminarabiose analogue maps appear almost identical, but are different in detail from the cellobiose analogue map. For the analogues of the (1 → 2)-β- and (1 → 3)-β-linked sophorose and laminarabiose, the two lowest energy minima are distributed one to each side of $\psi = 0°$ in the same trough region as is prominent on the corresponding disaccharide maps. For the analogue of the (1 → 4)-β-linked cellobiose, this region

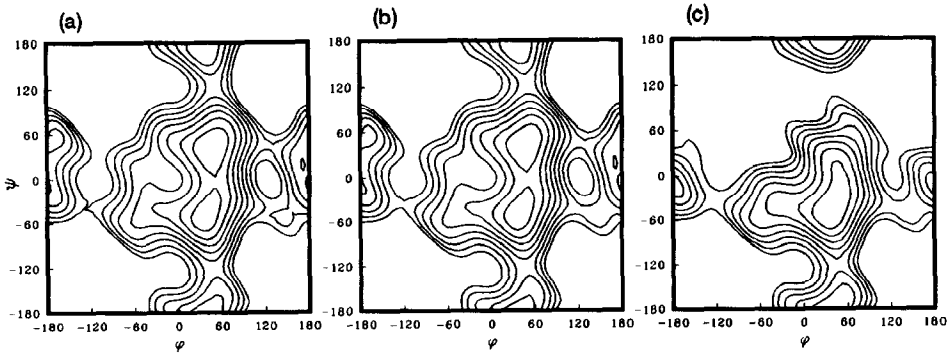

Fig. 9. MM3-generated relaxed-residue steric energy maps of equatorially–equatorially linked 3-(6-methyltetrahydropyran-2-yloxy)-6-methyltetrahydropyran (a), 4-(6-methyltetrahydropyran-2-yloxy)-6-methyltetrahydropyran (b), and 5-(6-methyltetrahydropyran-2-yloxy)-6-methyltetrahydropyran (c).

is condensed, with only a single minimum occurring at negative values of ψ. Similar traits are apparent on the disaccharide maps, as well as for the α-linked disaccharides and their analogues considered in our earlier work[11]. This shows that a bulky side-group attached one carbon atom away from the glycosidic bonds has an important influence on the conformational freedom of these molecules.

Comparison of modelling results with crystal structures.—Ohanessian et al. have reported a crystal structure for α-sophorose monohydrate[26]. The ϕ, ψ location of this structure, shown in Fig. 3, is in good agreement with the second lowest MM3

TABLE V

Steric energy minima for MM3-generated relaxed-residue analysis of the 6-methyltetrahydropyran analogues of sophorose, laminarabiose, and cellobiose

Structure	Location of minimum		Relaxed energy (kcal/mol)
	ϕ	ψ	
Equatorially–equatorially linked	46.5	40.8	20.57
3-(6-methyltetrahydropyran-	39.4	−51.8	20.90
2-yloxy)-6-methyltetrahydropyran	37.1	170.8	23.52
	−166.7	57.2	24.11
	−179.9	−9.9	24.42
	144.4	−54.7	27.27
Equatorially–equatorially linked	46.8	41.6	20.52
4-(6-methyltetrahydropyran-	37.5	−52.2	20.81
2-yloxy)-6-methyltetrahydropyran	37.2	169.6	23.47
	−167.0	57.4	24.09
	−179.3	−12.1	24.32
	145.5	−55.2	26.97
Equatorially–equatorially linked	36.8	−50.0	21.15
5-(6-methyltetrahydropyran-	39.9	177.8	24.16
2-yloxy)-6-methyltetrahydropyran	−178.6	−13.3	24.53

minimum found for α-sophorose. This MM3 minimum did not produce any significant inter-ring hydrogen bonds, and none occur within the crystal structure. The hydroxymethyl groups of the crystal structure are in a *gtgg* orientation, although modelling found the *gtgt* orientation to have less energy. Packing forces should influence these orientations in the crystal structure. The C-1–O-1–C-2′ valence angle is well reproduced. A comparison of selected geometric parameters for the anomeric and glycosidic regions for the global and second MM3 minimum with the crystal structure is given in Table VI. That the experimental structure agreed with the second lowest energy minimum and not the global minimum is not unrealistic, since the energy difference between these two minima is only 0.6 kcal/mol. Other disaccharide crystal structures are located in regions of the map as much as 1.5 kcal/mol above the MM3-modelled global minima[10,11], and crystals of larger oligosaccharides with similar disaccharide subunits are found in regions as much as 3 kcal/mol above their global minima. In addition, intermolecular packing forces and the water molecule present within the sophorose crystal structure are not accounted for by the MM3 algorithm.

A crystal structure for a hydrated anomeric mixture of laminarabiose has been reported by Takeda et al.[27]. The ϕ, ψ values of this structure are 28°, −38°, which are in good agreement with the MM3 global minima of the two anomers. This crystal conformer is shown on both maps in Fig. 5, and selected geometric parameters are compared in Table VII. The crystal glycosidic valence angle of 118.2° is large compared to the same angle in other equatorially–equatorially linked disaccharide crystals (113.6° in α-sophorose[26], 116.5° in β-lactose[28], 116.1° in β-cellobiose[29], 115.8° in methyl-β-cellobioside[30]), as well as when compared to the MM3-calculated angle (116.2°). Evidence exists that modelled disaccharide energies are not very sensitive to this angle[31]. A strong inter-ring hydrogen bond is found in the crystal structure between O-5 and H(O-4′) and is also predicted by MM3. In contrast, early rigid-monomer work suggested that an inter-ring hydrogen bond between O-2 and O-2′ was to be expected for laminarabiose[8]. The global minimum predicted by MM3 also indicates that a small interaction occurs between O-6 and H(O-4′), although the O–O distance is quite large (Table VII).

Crystal structures have been reported for β-cellobiose[29] and for a methyl β-cellobioside–methanol complex[30]. Their geometric properties are summarized in Table VIII. The ϕ, ψ values of these two structures are 42°, −18° for the first and 25°, −48° for the second. These values correspond closely with the lowest energy minima on the MM3 β-cellobiose maps and are shown in Fig. 7. Also shown are three pairs of ϕ, ψ values derived from X-ray fiber diffraction studies of cellulose[32–34]. These values lie along a diagonal line passing through ϕ, ψ values of 180°, −180° and −180°, 180° that represent structures having a twofold screw axis. These polysaccharide values also lie within the lowest-energy region of the map (< 2 kcal/mol) in a region between the two disaccharide crystal values. As shown in Table VIII, the C-1′–O-1′ bond calculated by MM3 is longer by an average of 0.0047 nm than that found in the two crystal structures containing the

TABLE VI

Selected bond lengths, valence angles, and torsional angles of α- and β-sophorose from MM3 calculations and crystallographic data

Bonds	MM3 model			Crystallographic data
	α-Sophorose	α-Sophorose (2nd minimum)	β-Sophorose	α-Sophorose monohydrate [a]
	Bond lengths (nm)			
C-1–C-2	0.1526	0.1526	0.1527	0.1530
C-1–O-1	0.1408	0.1407	0.1407	0.1403
C-1–O-5	0.1429	0.1428	0.1428	0.1423
C-5–O-5	0.1423	0.1423	0.1422	0.1438
C-1′–C-2′	0.1530	0.1528	0.1529	0.1524
C-1′–O-1′	0.1438	0.1430	0.1427	0.1418
C-1′–O-5′	0.1408	0.1420	0.1416	0.1422
C-2′–O-1	0.1426	0.1428	0.1430	0.1440
C-2′–C-3′	0.1528	0.1527	0.1529	0.1506
C-5′–O-5′	0.1424	0.1426	0.1423	0.1444
	Valence angles (degrees)			
C-1–O-1–C-2′	115.6	113.6	113.6	113.6
C-1–O-5–C-5	112.7	112.6	112.7	110.6
C-2–C-1–O-1	106.6	106.8	106.8	107.2
C-2–C-1–O-5	107.8	107.9	107.8	110.9
O-1–C-1–O-5	108.2	106.8	108.3	107.9
O-1–C-2′–C-1′	110.2	107.2	107.3	111.3
O-1–C-2′–C-3′	106.7	109.2	106.7	108.5
C-1′–O-5′–C-5′	115.2	114.5	113.1	115.1
C-2′–C-2′–O-1′	110.4	110.2	108.9	110.3
C-2′–C-1′–O-5′	110.0	109.2	108.7	109.2
O-1′–C-1′–O-5′	109.8	110.5	106.6	109.6
	Torsional angles (degrees)			
H(C-1)–C-1–O-1–C-2′	33.4	46.2	48.0	41.4
C-1–O-1–C-2′–H(C-2′)	−54.2	13.7	−8.3	20.8
C-1–O-1–C-2′–C-1′	66.8	132.2	113.3	98.0
C-1–O-1–C-2′–C-3′	−172.4	−107.9	−129.1	−139.7
C-2–C-1–O-5–C-5	−66.1	−66.2	−66.3	−64.2
C-5–O-5–C-1–O-1	179.0	178.6	178.5	178.7
O-1–C-2′–C-1′–O-1′	50.0	54.5	−71.4	57.7
O-5–C-1–O-1–C-2′	−89.6	−76.6	−74.9	−78.8
C-2′–C-1′–O-5′–C-5′	−59.5	−60.7	−65.4	−56.6
C-3′–C-2′–C-1′–O-1′	−68.1	−64.6	173.0	−63.0
C-5′–O-5′–C-1′–O-1′	62.2	60.6	177.3	64.3

[a] Ref. 26.

β-cellobiosyl moiety. The same discrepancy is found with the anomeric hydroxyl groups in glucose[15] and maltose[11] but not with the analogous group in sophorose, suggesting that MM3 poorly models the bond length between the anomeric carbon and oxygen in glucosyl residues not linked through their C-2 atoms to another residue. Table VIII shows, however, that the glycosidic valence angles of the MM3

TABLE VII

Selected bond lengths, valence angles, and torsional angles of α- and β-laminarabiose from MM3 calculations and crystallographic data

Bonds	MM3 model		Crystallographic data
	α-Laminarabiose	β-Laminarabiose	α:β (2:3)-Laminarabiose hydrate [a]
	Bond lengths (nm)		
C-1–C-2	0.1528	0.1527	0.1524
C-1–O-1	0.1408	0.1407	0.1387
C-5–O-5	0.1424	0.1424	0.1435
O-1–O-5	0.1429	0.1428	0.1445
O-1–C-3′	0.1427	0.1427	0.1431
C-1′–O-1′ (α)	0.1437		0.1271 [b]
C-1′–O-1′ (β)		0.1420	0.1340 [b]
C-1′–O-5′	0.1407	0.1424	0.1428
C-2′–C-3′	0.1529	0.1532	0.1517
C-3′–C-4′	0.1533	0.1534	0.1548
C-5′–O-5′	0.1424	0.1422	0.1431
	Valence angles (degrees)		
C-1–O-1–C-3′	116.2	116.1	118.2
C-1–O-5–C-5	113.0	112.9	112.5
C-2–C-1–O-5	107.6	107.8	108.8
C-2–C-1–O-1	106.7	106.3	110.5
O-1–C-1–O-5	108.4	108.7	106.7
O-1–C-3′–C-2′	104.8	105.1	105.7
O-1–C-3′–C-4′	111.4	110.5	112.0
C-1′–O-5′–C-5′	114.2	112.0	113.5
C-2′–C-1′–O-1′ (α)	110.5		117.3
C-2′–C-1′–O-1′ (β)		107.3	109.6
C-2′–C-1′–O-5′	108.8	108.1	109.1
C-2′–C-3′–C-4′	108.1	109.4	111.2
O-1′–C-1′–O-5′ (α)	110.5		110.5
O-1′–C-1′–O-5′ (β)		108.4	111.7
	Torsional angles (degrees)		
H(C-1)–C-1–O-1–C-3′	35.4	35.0	27.9
C-1–O-1–C-3′–H(C-3′)	−48.1	−42.3	−37.5
C-1–O-1–C-3′–C-2′	−166.9	−160.7	−161.0
C-1–O-1–C-3′–C-4′	76.5	81.4	77.7
C-2–C-1–O-5–C-5	−65.7	−65.7	−62.3
C-2–C-1–O-1–C-3′	156.5	155.8	148.3
O-5–C-1–O-1–C-3′	−87.8	−88.3	−93.6
C-2′–C-1′–O-5′–C-5′	−61.3	−66.8	−62.5
C-3′–C-2′–C-1′–O-1′	−64.7	175.2	177.6 (β)
C-5′–O-5′–C-1′–O-1′	60.1	177.2	176.2 (β)
	Intramolecular distances (nm)		
O-5 ··· H(O-4′)	0.1943	0.1906	0.2044
O-5 ··· O-4′	0.2664	0.2680	0.2786
O-6 ··· H(O-4′)	0.2295	0.2386	0.2627
O-6 ··· O-4′	0.3080	0.3121	0.3300

[a] Ref. 27. [b] Because of the α-β disorder, these values are not expected to be accurate.

TABLE VIII

Selected geometric characteristics of α- and β-cellobiose from MM3 calculations and crystallographic data

Bonds	MM3 model			Crystallographic data	
	α-Cellobiose	β-Cellobiose	β-Cellobiose (2nd minimum)	β-Cellobiose [a]	Methyl β-cellobiose-methanol [b]
	Bond lengths (nm)				
C-1–C-2	0.1527	0.1528	0.1527	0.1525	0.1526
C-1–O-1	0.1408	0.1408	0.1408	0.1397	0.1390
C-1–O-5	0.1427	0.1429	0.1428	0.1425	0.1432
C-5–O-5	0.1423	0.1424	0.1423	0.1436	0.1430
O-1–C-4′	0.1430	0.1428	0.1430	0.1446	0.1437
C-3′–C-4′	0.1530	0.1534	0.1531	0.1530	0.1533
C-4′–C-5′	0.1532	0.1537	0.1533	0.1527	0.1526
C-1′–O-1′	0.1437	0.1427	0.1427	0.1381	0.1379
C-1′–O-5′	0.1408	0.1414	0.1415	0.1435	0.1434
C-5′–O-5′	0.1426	0.1423	0.1424	0.1437	0.1432
	Valence angles (degrees)				
C-1–O-1–C-4′	113.9	116.4	113.8	116.1	115.8
C-1–O-5–C-5	112.7	113.1	112.7	112.4	111.1
C-2–C-1–O-1	107.0	106.2	107.0	109.0	110.4
C-2–C-1–O-5	107.6	107.6	107.6	108.3	107.4
O-1–C-1–O-5	108.6	108.6	108.6	107.4	107.6
O-1–C-4′–C-3′	107.4	110.6	107.5	109.0	111.5
O-1–C-4′–C-5′	107.2	105.2	107.2	106.4	107.2
C-1′–O-5′–C-5′	114.8	112.4	112.9	113.5	111.3
C-2′–C-1′–O-1′	110.4	108.5	108.4	110.2	107.0
C-2′–C-1′–O-5′	109.2	107.7	108.4	109.3	108.7
C-3′–C-4′–C-5′	109.6	109.8	109.7	112.3	109.1
O-1′–C-1′–O-5′	110.0	107.3	107.2	109.3	108.3
	Torsional angles (degrees)				
H(C-1)–C-1–O-1–C-2′	50.4	36.0	50.5	42	25
C-1–O-1–C-2′–H(C-2′)	−10.7	−46.2	−10.7	−18	−48
C-1–O-1–C-4′–C-3′	111.0	77.3	110.9	73.6	80.3
C-1–O-1–C-4′–C-5′	−131.2	−164.3	−131.2	−132.3	−160.7
C-2–C-1–O-1–C-4′	171.5	157.1	171.7	166.6	152.0
C-2–C-1–O-5–C-5	−66.6	−65.6	−66.5	−65.7	−69.1
C-5–O-5–C-1–O-1	178.0	179.3	178.0	176.7	172.0
O-5–C-1–O-1–C-4′	−72.6	−87.1	−72.5	−76.3	−88.9
C-2′–C-1′–O-5′–C-5′	−60.2	−66.9	−65.6	−63.5	−64.3
C-3′–C-2′–C-1′–O-1′	−61.2	174.4	173.9	175.1	167.8
C-5′–O-5′–C-1′–O-1′	61.0	176.5	177.7	175.6	179.8
	Intramolecular distances (nm)				
O-5 · · · O-3′	0.2682	0.2661	0.2684	0.2767	0.2762
O-6 · · · O-3′	0.3480	0.3094	0.3480	0.3120	0.2914

[a] Ref. 29. [b] Ref. 30. Values of torsion angles not given in the article were calculated from a chiral inversion because the original structure was inadvertantly reported as the L-form.

model for β-cellobiose are in good agreement with the two experimental values. The methyl β-cellobioside crystal has a bifurcated hydrogen bond where H(O-3′) is linked to both O-5 and O-6. The former bond is much stronger than the latter, as is indicated by the O–O distances shown in Table V. This hydrogen bonding pattern is also seen in the corresponding MM3 global minimum of β-cellobiose, and the O–O distances are in good agreement, although the O-6 to H(O-3′) bonding is very weak. For the β-cellobiose crystal structure, the only inter-ring hydrogen bond is between O-5 and H(O-3′). The ϕ, ψ values of this structure are closer to the second MM3 minimum of cellobiose, and the same hydrogen bond occurs in this model. MM3 also finds a very weak interaction between H(O-6) and O-3′, with a correspondingly large O–O distance. Of the exocyclic orientations considered, the *gt* orientation of the hydroxymethyl groups have the lowest energy. The orientation of the these groups is *gtgt* and *gtgg* for the for the β-cellobiose and methyl β-cellobioside crystal structures, respectively. In the latter structure, the O-6′ oxygen atom accepts a hydroxyl hydrogen atom from the hydroxyl group of the methanol moiety.

The MM3 force field and the more complete collection of starting models result in maps that have important differences from maps made with MM2(85)[5–7]. In particular, the energy barrier separating the cellobiose and methyl cellobioside structures is 1.7 kcal/mol lower. This leaves only a small penalty for the 2_1 structures of cellulose (0.2 kcal/mol) compared to structures based on either or both of the two minima. Such a small energy associated with 2_1 structures could easily be overcome by crystal-packing forces. Another difference is that the MM3 energies of the structures near $\phi = 180°$ or $\psi = 180°$ are higher than MM2(85) energies[5–7]. These structures, which lead to folded-chain cellulose or to helices similar to V-amylose, are now seen as somewhat less likely.

This article closes a particular series of calculations on the simple disaccharides composed of two D-glucosyl residues connected by two bonds. Several limitations affected these calculations, the most important of which is probably the use of $\epsilon = 4$, which diminishes the strength of electrostatic interactions such as hydrogen bonding. It was chosen because our best information on conformations comes from crystal structures, and within the MM3 formalism this adjustment is the chosen way to compensate for the presence of neighboring molecules. Preliminary calculations show that lower dielectric constants have a strong effect (work in progress). Other limitations were the use of only a limited number of starting conformations of the rotatable exo-cyclic groups and the exclusion of ring forms other than the widely accepted $^4C_1$ shape. We stress that the starting arrangements of rotatable groups were often disrupted during optimization, and that the conformations indicated in Figs. 4, 6, and 8 are starting rather than final structures. This will have some effect on the calculated partition functions. Based on other studies underway, we do not believe that these limitations have a serious impact on the character of the calculated maps. The grid size, 20° in both ϕ and ψ, was adequate for these relaxed-residue studies.

Given that a single hydrogen bond can have a strength of 5 kcal/mol or more, it is remarkable that none of the linkages observed in the α- or β-linked D-glucosyl disaccharide crystal structures is distorted by packing and hydrogen-bonding forces in excess of 3 kcal/mol. At least for D-glucopyranosyl rings, it appears that MM3 is very capable of predicting like structures and ruling out unlikely alternatives. Not only are the energies of models having observed crystal conformers low, but the shape of the low-energy regions matches well the distributions of observed crystal structures when, as in the case of maltose, many observations are available. This is not yet the case for the sucrose molecule, as the sucrosyl moiety in crystalline raffinose has a glycosidic conformational energy 5.5 kcal/mol above that of the calculated minimum (work in progress). In addition, the population of observed structures with sucrosyl linkages appears to be shifted 20° in the ψ-direction from the predicted low-energy region[35].

The averaged energy values seem to be quite reasonable and also help to explain the observed disaccharide distributions. By the device of using a number of starting models, the predicted energy distributions can be used to describe population densities of conformers. This type of calculation will be of increasing interest as emphasis shifts toward understanding saccharide solution properties. Considering as many possible side-group orientations as was done here in constructing a conformational map may be a plausible alternative to conducting molecular dynamics studies. Although the improvements in the MM3 force field over its predecessors are apparently responsible for most of the changes in character from earlier maps, some of the changes in the fine details arise from the consideration of a large number of side-group orientations. Both changes improved the fit of the model with experimental data.

One lesson from this work is that D-glucosyl disaccharides are fairly flexible, with torsional angles spanning as much as 100° for the equatorial linkages, both by experiment and by calculation. Therefore, a single structure from a diffraction experiment can differ substantially from the minimum predicted by calculation, and it is perhaps fortuitous that so many of the crystal structures we used for comparison fall so close to the minima in calculated energy.

CONCLUSION

Relaxed-residue MM3 energy maps are presented for the two anomeric forms of sophorose, laminarabiose, and cellobiose. The relative positions of the low-energy regions illustrate the influence of the exo-anomeric effect. The similarities of the disaccharide and tetrahydropyran analogue maps show the importance of the equatorial–equatorial glycosidic linkages in determining molecular conformation. As is most clearly demonstrated on the analogue maps, the placement of a relatively small chemical group one carbon atom removed from the glycosidic region has some influence on the low-energy regions of the map. Differences between the disaccharide anomers are most pronounced for sophorose, where the

glycosidic bond is closest to the anomeric region of the reducing ring. Glycosidic torsional angles of crystal structures are in good agreement with the calculated low-energy conformations.

REFERENCES

1 S. Melberg and K. Rasmussen, *Carbohydr. Res.*, 71 (1979) 25–34.
2 G.M. Lipkind, V.E. Verovsky, and N.K. Kochetkov, *Carbohydr. Res.*, 133 (1984) 1–13.
3 B. Henrissat, S. Pérez, I. Tvaroška, and W.T. Winter, *ACS Symp. Ser.*, 340 (1987) 38–67.
4 A.D. French, *Biopolymers*, 27 (1988) 1519–1525.
5 A.D. French, *Carbohydr. Res.*, 188 (1989) 206–211.
6 A.D. French, in C. Schuerch (Ed.), *Cellulose and Wood—Chemistry and Technology*, Wiley, New York, 1989, pp. 103–118.
7 A.D. French, V.H. Tran, and S. Pérez, *ACS Symp. Ser.*, 430 (1990) 191–211.
8 B.K. Sathyanarayana and V.S.R. Rao, *Biopolymers*, 10 (1971) 1605–1615.
9 B.K. Sathyanarayana and V.S.R. Rao, *Biopolymers*, 11 (1972) 1379–1394.
10 M.K. Dowd, A.D. French, and P.J. Reilly, *J. Comput. Chem.*, 13 (1992) 102–114.
11 M.K. Dowd, J. Zeng, A.D. French, and P.J. Reilly, *Carbohydr Res.*, 230 (1992) 223–244.
12 N.L. Allinger, Y.H. Yuh, and J.H. Lii, *J. Am. Chem. Soc.*, 111 (1989) 8551–8566.
13 J.H. Lii and N.L. Allinger, *J. Am. Chem. Soc.*, 111 (1989) 8566–8575.
14 N.L. Allinger, M. Rahman, and J.H. Lii, *J. Am. Chem. Soc.*, 112 (1990) 8293–8307.
15 A.D. French, R.S. Rowland, and N.L. Allinger, *ACS Symp. Ser.*, 430 (1990) 120–140.
16 R.H. Marchessault and S. Pérez, *Biopolymers*, 18 (1979) 2369–2374.
17 A. De Bruyn and M. Anteunis, *Carbohydr. Res.*, 47 (1976) 311–314.
18 Y. Nishida, H. Ohrui, and H. Meguro, *Tetrahedron Lett.*, 25 (1984) 1575–1578.
19 S.N. Ha, J. Madsen, and J.W. Brady, *Biopolymers*, 27 (1988) 1927–1952.
20 I. Tvaroška and L. Václavík, *Carbohydr. Res.*, 160 (1987) 137–149.
21 T. Usui, M. Yokoyama, N. Yamanaka, K. Matsuda, K. Tuzimura, H. Sugiyama, and S. Seto, *Carbohydr. Res.*, 33 (1974) 105–116.
22 J. Haverkamp, J.P. Kamerling, and J.F.G. Vliegenthart, *J. Chromatogr.*, 59 (1971) 281–287.
23 Z.L. Nikolov and P.J. Reilly, *J. Chromatogr.*, 254 (1983) 157–162.
24 T. Toba and S. Adachi, *J. Chromatogr.*, 135 (1977) 411–417.
25 I. Tvaroška, *Biopolymers*, 23 (1984) 1951–1960.
26 P.J. Ohanessian, F. Longchambon, and F. Arene, *Acta Crystallogr., Ser. B*, 34 (1978) 3666–3671.
27 H. Takeda, N. Yasuoka, and N. Kasai, *Carbohydr. Res.*, 53 (1977) 137–152.
28 K. Hirotsu and A. Shimada, *Bull. Chem. Soc. Jpn.*, 47 (1974) 1872–1879.
29 S.S.C. Chu and G.A. Jeffrey, *Acta Crystallogr., Ser. B*, 24 (1968) 830–838.
30 J.T. Ham and D.G. Williams, *Acta Crystallogr., Ser. B*, 26 (1970) 1373–1383.
31 C.H. du Penhoat, A. Imberty, N. Roques, V. Michon, J. Mentech, G. Descotes, and S.Pérez, *J. Am. Chem. Soc.*, 113 (1991) 3720–3727.
32 K.H. Gardner and J. Blackwell, *Biopolymers*, 13 (1974) 1975–2001.
33 A.D. French, *Carbohydr. Res.*, 61 (1978) 67–80.
34 C. Woodcock and A. Sarko, *Macromolecules*, 13 (1980) 1183–1187.
35 S. Pérez, C. Meyer, A. Imberty, and A. French, in G. Birch and M. Mathlouthi (Eds.), *Sweet Taste Chemoreception*, Elsevier, Amsterdam, in press.